

# Discovery of 16 Nearby Brown Dwarf Candidates in WISE Preliminary Release Data

October 14, 2011

## Abstract

We report a discovery of sixteen nearby brown dwarf candidates and seven temperature-specific ( $\sim 200$  K  $\sim 500$  K) populations ( $\sim 102$  sources) in the WISE Preliminary Release Data. Four of the candidates are between 285 K and 400 K, temperatures akin to that of Earth. Eleven of the candidates were identified by querying WISE with magnitudes based on a pure blackbody spectrum assumption; the remaining five resulted from Monte Carlo variant queries generated through application of randomization factors of 50% and 20% to the blackbody magnitudes of the low ( $\sim 2.8 - \sim 5.4\mu\text{m}$ ) and high (7 - 28  $\mu\text{m}$ ) wavelength WISE band passes, respectively. The correlation between the spectra of nine of the blackbody candidates and the temperature-equivalent blackbody spectra was within 1%. The respective concurrence of the remaining two was within 15%. The Monte Carlo queries also identified local interstellar brown dwarf populations ( $\sim 102$  sources) for 7 evenly incremented temperatures between 200 K and 500 K, inclusively. The ratios of the spectra of the 7 Monte Carlo query brown dwarf population returns to band 1 flux values were modeled as third-degree polynomial functions of wavelength.

# Discovery of 16 Nearby Brown Dwarf Candidates in WISE Preliminary Release Data

Govinda Dasu, The Harker School, San Jose, CA

October 16, 2011

## 1 Introduction

The research endeavor involved a search for the nearest brown dwarf<sup>\*1</sup> candidates and a search for the hypothetical cool outer-solar-system brown dwarf, commonly referred to as “Planet X”, in the WISE (Wise Infrared Survey Explorer) telescope preliminary release data. The work was inspired by the recent discovery of the coolest known brown dwarf [1] (300 K) (Burgasser et al.), which is at a temperature akin to that of Planet Earth. We sought populations of such cool brown dwarfs, with a focus on identification of the nearest candidates, particularly those within our solar system ( $d < 1 \text{ ly}$ )<sup>2</sup>. The procedure involved the blackbody modeling of 200 - 800 K cool brown dwarfs and the subsequent generation of blackbody-adherent and blackbody-variant (Monte Carlo<sup>\*</sup>) magnitude difference constraint queries. The queries were submitted to the WISE preliminary release source catalog covering 57% of the celestial plane. The blackbody-adherent queries returned eleven legitimate candidates. The blackbody-variant queries returned populations of brown dwarfs at individual temperature ranges throughout the sky that followed an isotropic<sup>\*</sup> distribution in the 2D celestial plane and the 3D celestial sphere. The closest of those candidates were recognized as the nearest brown dwarf candidates. However, like the blackbody-spectrum-adherent candidates, the Monte Carlo near brown dwarf candidates can only be confirmed after proper motion and parallax tests upon the second epoch data release.

In this study, it was assumed that all celestial brown dwarfs of a given temperature would have identical spectra and that the brown dwarfs would be  $\sim 1R_J$ <sup>\*</sup> in size. It was also assumed that the brown dwarfs, because of their ammonia, methane and water clouds, would have absorption bands, causing their apparent magnitude<sup>\*</sup> difference between bands<sup>\*</sup> 1 and 2 to be at least 2.5 V. It was hypothesized that all interstellar brown dwarfs of a given temperature could be found in the WISE telescope data by either querying magnitudes derived from theory based on Planck’s Blackbody function or querying magnitudes based off of a Monte Carlo variation of the blackbody queries. The Monte Carlo generation process would employ blackbody values, but add significant randomization ( 50%) to band 1 and 2 magnitudes and minimal randomization ( 20%) to band 3 and 4 magnitudes. This “query spamming” technique would allow for the correct spectra to result in a spike of candidates from a celestial population of identical brown dwarfs.

John Whitmire and Daniel Matese’s paper, “Persistent Evidence of a Jovian Mass Solar Companion in the Oort Cloud [2]” provided inspiration for our research in its assertion that the “wide-binary Jovian mass companion”, or the hypothetical Planet X, exists and can be identified with the release of the WISE telescope data. Matese and Whitmire employed theoretical physical and chemical complex system models to assert the existence of a particular Jovian companion, termed by them “Tyche”, within the solar system [2]. Our method devised for isolation of cool brown dwarf candidates in WISE preliminary release data employed many of the same techniques as those of Scholz et al. in the paper Two very nearby ( $d \approx 5 \text{ pc}$ ) ultracool brown dwarfs detected by their large proper motions from WISE, 2MASS, and SDSS data [3]. Specifically, in their paper, WISE source catalogs were queried by band difference constraints that anticipate an expected

---

<sup>1</sup>Definitions for starred (\*) terms are available in the glossary at the end of the paper.

<sup>2</sup>Specification of distance less than one light year away

spectra of the sought dwarf, mandating, for instance,  $w_1 - w_2 > 2$  and  $w_2 - w_3 < 2.5$  V\*. While Scholz et. al employed J. Burgasser’s theoretical spectral models, calculated from multi-parameter complex system simulations, we generated several magnitude difference constraint queries with Monte Carlo Randomization variants of a standard blackbody spectra as described in Section 2. After querying, Scholz et al. assessed their 98 candidates for sufficient proper motion and parallax through comparison with 2MASS data, confirming 2 near brown dwarfs (WISE J0254+0223 and WISE J1741+2553). Our research procedure included this step of comparison with 2MASS data for six of the sixteen candidates, but the rest of the candidates had magnitudes that were not within the limiting magnitudes\* of 2MASS, making proper motion and parallax calculations possible only after release of WISE second epoch data.

While the primary purpose of our research was to minimize dependence upon theoretical models of cool brown dwarfs, it was found in the literature that recognition of certain imminent phenomenon of known brown dwarfs was necessary. The paper *Beyond the T Dwarfs: Theoretical Spectra, Colors, and Detectability of the Coolest Brown Dwarfs* [4] described the presence of H<sub>2</sub>O, CH<sub>4</sub>, and NH<sub>3</sub> molecular bands in all known cool brown dwarfs of temperature  $\sim 130$  to  $\sim 800$  K. These bands would result in absorption of electromagnetic frequencies in the first band pass of the WISE telescope ( $2.8\mu\text{m} - 3.8\mu\text{m}$ ) causing a significant magnitude difference between  $w_1$  and  $w_2$ . This difference was recognized as a parameter in the experiment, and the  $w_1 - w_2$  apparent magnitude difference constraint was set at a minimum of 2 V.

The rest of the investigated literature confirmed the findings of the above. For instance,  $\widehat{\text{FIRE}}$  Spectroscopy of Five Late-Type T Dwarfs Discovered with the Wide-Field Infrared Survey Explorer [5] (Adam Burgasser et al.) confirmed the legitimacy of the assumption of large absorption bands in band 1 of WISE as well as the procedure of isolating candidates by querying magnitude constraints and subsequently performing parallax and proper motion checks. The paper *Preliminary Results from NEOWISE: An Enhancement to the Wide-field Infrared Survey Explorer for Solar System Science*[6] provided information about the second batch of the WISE data which, when released in March 2012, will be able to confirm the candidates found by this research endeavor. The paper *Transformations between WISE, 2MASS, SDSS and BVRI photometric systems* [7] provided information on WISE limiting magnitudes and how to discern whether a WISE candidate would be detectable by 2MASS. This tool proved useful because five of the blackbody candidates found were not visible in 2MASS based on their magnitudes in WISE and were therefore reserved for potential confirmation with the 2012 release.

## 2 Materials and Methods: Theoretical Calculations and Procedures

In order to detect an interstellar brown dwarf which has a radius of  $0.90R_J$  to  $1.10R_J$  and an effective blackbody temperature of 200 K to 800 K, apparent magnitude (V) ranges were derived from first principles and expressed as SQL\* queries that were fed to the WISE Preliminary Release Source Catalog [8]. Using equatorial coordinates of the sources from ASCII\* tables of information provided by the Catalog, specific FITS files of the astronomical objects were obtained from the NASA/IPAC Infrared Science Archive [9] and manually assessed for exhibition of low-temperature planetary phenomenon such as un-stretched circular shape and point source symmetry in all four bands. The queries themselves comprised 35 astronomical magnitude constraints derived from 35 evenly distributed temperature ranges between 100 K and 800 K independent of distance and radius. For each candidate of each search result, the apparent brightness magnitudes (V) in the four bands of the WISE telescope were extracted from the ASCII table of source information. The magnitudes and standard deviations of each source were interpreted as indicators of the temperature, radius, and distance to the candidate planet.

In Mathematica [10], Planck’s law for the intensity of blackbody radiation (Eq. 1) was defined, expressing power per unit area per unit solid angle per unit wavelength (erg / s / cm<sup>2</sup> / steradian / cm) as a function of light wavelength (cm) and temperature (K) of the blackbody.

$$I(\lambda, T) = \frac{2hc^2}{\lambda^5} \frac{1}{e^{\frac{hc}{\lambda kT}} - 1} \quad (1)$$

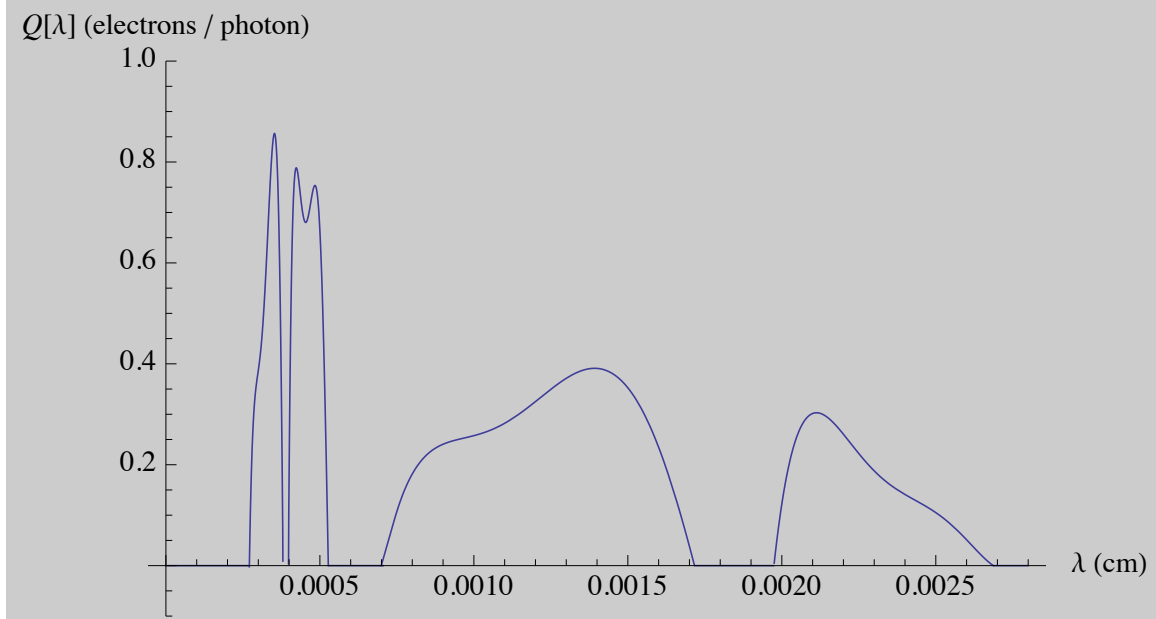


Figure 1: Plot of the WISE CCD Quantum Efficiency Function

The WISE telescope quantum efficiency (electrons / photon) was then modeled as a function of wavelength, expressing the number of electrons released by the WISE CCD (charged coupled device) per photon to which it comes in contact. Specifically, a digital image [11] of a logarithmically scaled plot of the WISE quantum efficiency function was manually converted into a finite set of data points through use of *Logger Pro Photo Analysis Tools*[12]. The finite set of data points in the form of (wavelength  $\lambda$ , quantum efficiency  $Q(\lambda)$ ) were sorted by wavelength until sufficient data points existed for each of the four WISE band passes such that the individual polynomial fitting of each of the data sets (shown together in Figure 1) proved feasible. The models of quantum efficiency in WISE bands 1, 2, 3, and 4 are expressed in Eq. 2, 3, 4, and 5 respectively, where units of the coefficients are in electrons, per photon, per centimeter (cm is raised to the same order to which  $\lambda$  is raised). Unit analysis shows that the output for all four functions defined below is in electrons per photon.

$$Q_1(\lambda) = -2201.26 + 3.139 \times 10^7 \lambda - 1.761 \times 10^{11} \lambda^2 + 4.84482 \times 10^{14} (e^- / \gamma / cm^3) \lambda^3 - 6.486 \times 10^{17} \lambda^4 + 3.350 \times 10^{20} \lambda^5 \quad (2)$$

$$Q_2(\lambda) = -2.15 \times 10^4 + 2.279 \times 10^9 \lambda - 9.631 \times 10^{11} \lambda^2 + 2.02938 \times 10^{15} \lambda^3 - 2.131 \times 10^{18} \lambda^4 + 8.926 \times 10^{20} \lambda^5 \quad (3)$$

$$Q_3(\lambda) = -30.092 + 1.276 \times 10^5 \lambda - 2.107 \times 10^8 \lambda^2 + 1.70165 \times 10^{11} \lambda^3 - 6.676 \times 10^{13} \lambda^4 + 1.014 \times 10^{16} \lambda^5 \quad (4)$$

$$Q_4(\lambda) = -3.995 \times 10^3 + 8.31868 \times 10^6 \lambda - 6.912 \times 10^9 \lambda^2 + 2.86466 \times 10^{12} \lambda^3 - 5.923 \times 10^{14} \lambda^4 + 4.887 \times 10^{16} \lambda^5 \quad (5)$$

In order to calculate the theoretical number of electrons released given the flux and band pass function, the Quantum Energy function giving the energy (ergs) of a photon of a given wavelength, was defined:

$$E(\lambda) = \frac{hc}{\lambda} \quad (6)$$

The number of electrons per second released by the WISE CCD per unit wavelength (electrons / s / cm) was expressed as  $N(\lambda, T)$  (Eq. 7), the product of the quantum efficiency function  $Q(\lambda)$  and the intensity function  $I(\lambda, T)$  divided by the energy of each captured photon energy,  $E(\lambda)$ .

$$N(\lambda, T) = \frac{I(\lambda, T) \times Q(\lambda)}{E(\lambda)} \quad (7)$$

$N(\lambda, T)$  was then multiplied with  $4\pi$  (Eq. 8) which was determined to be the solid Angle factor of a sphere.

$$N_1(\lambda, T) = 4\pi N(\lambda, T) \quad (8)$$

$N_1(\lambda, T)$  (electrons / s / cm<sup>2</sup> / cm), expressing electrons per second per unit wavelength was again multiplied with the area of the planet (cm<sup>2</sup>) as a function of its radius  $r$  (in  $R_J$ ) (Eq. 9) and with the fraction of the celestial sphere covered by the WISE telescope as a function of the distance (AU) to the candidate and WISE instrumentation constants, namely the radius of the primary mirror (20 cm) (Eq. refdistance).

$$A_p(r) = 4\pi r^2 \quad (9)$$

$$f(d) = \frac{\pi(20)^2}{4\pi(d \times 1.4958 \times 10^{13})^2} \quad (10)$$

$$N_2(\lambda, T, d, r) = N_1(\lambda, T) \times A_p(r) \times f(d) \quad (11)$$

The product expression (Eq. 11),  $N_2(\lambda, T, d, r)$  (electrons/s/cm), was integrated over the four WISE band passes producing four functions,  $B_1(T, d, r)$ ,  $B_2(T, d, r)$ ,  $B_3(T, d, r)$ ,  $B_4(T, d, r)$ , that expressed the theoretical number of electrons released by the WISE CCD per second as a function of the astronomical object's radius, distance away, and temperature (Eq. 12, 13, 14, and 15).

$$B_1(T, d, r) = \int_{\lambda_{\min}^1}^{\lambda_{\max}^1} N_2(\lambda, T, d, r) d\lambda \quad (12)$$

$$B_2(T, d, r) = \int_{\lambda_{\min}^2}^{\lambda_{\max}^2} N_2(\lambda, T, d, r) d\lambda \quad (13)$$

$$B_3(T, d, r) = \int_{\lambda_{\min}^3}^{\lambda_{\max}^3} N_2(\lambda, T, d, r) d\lambda \quad (14)$$

$$B_4(T, d, r) = \int_{\lambda_{\min}^4}^{\lambda_{\max}^4} N_2(\lambda, T, d, r) d\lambda \quad (15)$$

According to the WISE manual [9], source apparent magnitudes were calculated by the following formula, a negative constant factor times the log of the ratio of the electrons per second released by the CCD due to an observed object and the electrons per second released by the CCD due to the star Vega:

$$M(e_1, e_2) = -2.5 \log_{10}\left(\frac{e_1}{e_2}\right) \quad (16)$$

The known radius, distance to and temperature of Vega were entered into functions  $B_1$ ,  $B_2$ ,  $B_3$  and  $B_4$  to find the theoretical number of electrons released by the WISE CCD per second for each band due to Vega. The calibrated apparent magnitudes of an object given its temperature  $T$ , radius  $r$ , and distance away  $d$  were modeled as  $M_1(T, d, r)$ ,  $M_2(T, d, r)$ ,  $M_3(T, d, r)$  and  $M_4(T, d, r)$  (Eq. 17, 18, 19, and 20):

$$M_1(T, d, r) = M(B_1(T, d, r), B_1(T_v, d_v, r_v)) \quad (17)$$

$$M_2(T, d, r) = M(B_2(T, d, r), B_2(T_v, d_v, r_v)) \quad (18)$$

$$M_3(T, d, r) = M(B_3(T, d, r), B_3(T_v, d_v, r_v)) \quad (19)$$

$$M_4(T, d, r) = M(B_4(T, d, r), B_4(T_v, d_v, r_v)) \quad (20)$$

With the  $M$  functions, a set of magnitude constraint queries was generated to test for all cool blackbodies ( $200 \text{ K} < T < 800 \text{ K}$ ) at any distance away in the WISE-perceivable universe. This test was achieved by querying with the difference in the band magnitudes rather than by the values of the band magnitudes themselves. It was observed that the distance and planet radius parameters had negligible effect on band magnitude differences. Therefore, arbitrary constants for distance and planet radius, 10000 AU and 1.0 RJ, were placed into the function generating query strings that varied by temperature alone. Because the magnitude differences among the bands didn't vary as a result of distance and radius alteration, the query strings, while "designed" for objects within a given temperature range at 10000 AU and of 1.0 RJ, would test for any blackbody within the given temperature range at any distance and any radius. It is, however, well known that no single blackbody or near blackbody of temperature  $\sim 200 \text{ K}$  to  $\sim 800 \text{ K}$  is likely to be of radius significantly different from  $1.0R_J$  because the equation of state for a degenerate Hydrogen-Helium mixture mandates a stable radius of  $1.0R_J$  [2].

In addition, a set of Monte Carlo randomized variant queries was also generated based on their temperature-respective blackbody queries. Specifically, the query magnitude constraints were designed such that the theoretical sum of the flux in all four bands would be equivalent to the blackbody sum, but the distribution within the four bands would be, to some degree, arbitrary. The degree of variance was constrained by two assumptions: First, in bands 1 and 2, the randomized query magnitudes were required to be within 50% of the blackbody query magnitudes. Second, in bands 3 and 4, the randomized query magnitudes were required to be within 20% of the blackbody query magnitudes. To test the hypothesis that brown dwarfs of a population share identical spectra, it was assumed that among the 400 randomized queries for each of the seven evenly distributed temperatures (200 K - 500 K), the queries with an unusually large number of candidates, or a spike, would connote a collection of brown dwarfs. The queries that resulted in a small or negligible number of candidates would be considered containers of background object mimics.

### 3 Results

The WISE Preliminary Release Source Catalog returned 132 point sources (of 257,310,278 total) that met the magnitude difference constraints of the 35 blackbody queries entered. Of the 132 sources, 44 were unaffected by contamination from artifacts such as diffractions spikes (of nearby stars), scattered-light halos, optical ghosts, and latent images. Of the 44 unaffected, only eleven candidates had undamaged FITS files extracted from IRSA in which a distinct point source could be clearly recognized with the naked eye. For the eleven candidates, the temperature and distance were calculated assuming a radius of  $1.0 \pm 0.1R_J$  for all candidates (Table 3).

Of the eleven candidates, as is evident from Table 3, only candidates 1 and 3 can be considered to lie within the confines of our solar system ( $d < 60,000 \text{ AU}$ ). To determine whether the objects were true solar system planets or background mimics, the parallax shift in the angular position of the candidate object between the given WISE epoch and another epoch would be necessary. Unfortunately, no second epoch data were available. The second epoch data for the WISE telescope will be released in March 2012, at which time, these eleven candidates can either be confirmed or discarded. The following relation will be used to determine the parallax:

Table 1: List of 11 unaffected candidates with undamaged fits images

#	RA (°)	DEC (°)	T (K)	d (AU)
1	87.516	-73.332	285 ± 16	33178 +3570/-3521
2	246.084	-5.214	374.551 +4.6/-22	231283 +7276/-36098
3	286.578	15.124	420 ± 22	21194 +2286/-2254
4	84.048	-74.077	526 +21/-22	131629 +14988/-14632
5	83.842	-70.658	657 +34/-36	158450 +18450/-17934
6	81.029	-71.961	698 +12/-9	158563 +18443/-17928
7	177.977	-53.139	723 +36/-32	97436 +11306/-10995
8	86.918	- 72.813	716 +15/-11	167750 +19790/-19181
9	90.236	- 71.814	739 +10/-13	190828 +22115/-21513
10	85.629	- 71.783	760 +11/-14	185024 +21380/-20803
11	83.842	-70.658	767 +49/-63	158450 + 6843/- 23210

Table 2: Shift speed for each candidate compared with 2MASS Data

#	WISE		2MASS		Epoch	Shift Speed (arcsec / yr)
	RA (°)	DEC (°)	RA (°)	DEC (°)	Diff. (yr)	
5	83.84245	-70.65855	83.84251	-70.65856	10.175	0.0208
6	81.02947	-71.96143	81.02943	-71.96144	11.372	0.0131
7	177.97737	-53.13954	177.97733	-53.13954	9.847	0.0151
8	86.91856	- 72.81357	86.91859	-72.81348	11.337	0.0309
9	90.23664	- 71.81455	90.23663	-71.81455	11.397	0.00425
10	85.62966	- 71.78303	85.62967	-71.78300	12.019	0.0105

$$p(n, d) = \sin^{-1} \frac{\sqrt{2 - 2 \cos(2\pi n)}}{d} \quad (21)$$

Given the distance  $d$ , the time difference between the two epochs in days ( $n$ ), and the parallax relation (Eq. 21), we calculated that for candidates 1 and 3 respectively, 12.4338 (+0.738097/-0.603959) arcsec and 19.4652 (+2.31642/-1.89505) arcsec of parallax would be expected for an epoch separation, 180 days. The experimental value, when available, will have to be compared to this theoretical value calculated.

The nine candidates that were not solar-system objects were tested as extra-solar brown dwarf candidates. It was assumed that the plane-of-the-sky velocities were sampled from a 2D gaussian distribution with a standard deviation  $\sigma \approx 25$  km/s. The assumption implied that true extra-solar-system brown dwarfs would likely have an apparent positional shift in WISE data due to the relative motion of their system with respect to our sun. The  $\sim 25$  km/s shift would be equivalent to a  $\sim 42$  arcsec shift per year.

Candidates 5 through 10 were determined to be of a temperature large enough such that they would appear in at least one of the three 2MASS telescope band passes [13] given the 2MASS limiting magnitude of 14 [13].

After comparison with the 2MASS data taken approximately 12 years before the WISE survey, it was found (Table 2) that none of the six candidates exhibited sufficient proper motion shift ( $s > 42$  arcsec/yr). Therefore it was concluded that the probability of the six candidates being true brown dwarfs is equivalent to the probability that the relative motion of our sun with respect to the systems of the eight candidates is less than 25 km/s. The latter probability was determined to be small though not negligible enough for the rejection of the candidates. Because candidates 1 through 4 and 11 could not be detected by 2MASS, the same positional comparisons can only be done with the second release WISE epoch data once available.

The Monte Carlo Randomization technique produced a more complex set of candidates to be analyzed.

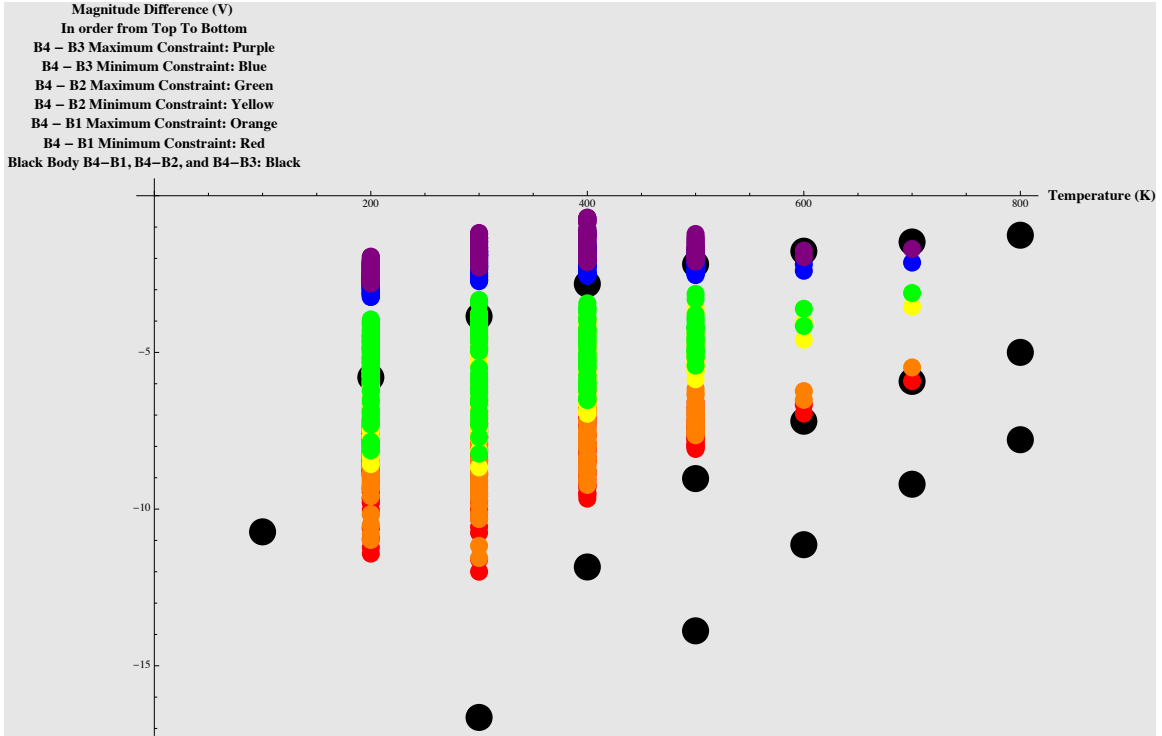


Figure 2: Plot of Query Magnitude Difference Ranges that returned candidates vs. Temperature

Figure 2 displays the  $b_4 - b_1$ ,  $b_4 - b_3$ , and  $b_4 - b_1^*$  magnitude difference constraints that produced candidates. As expected, candidates displayed blackbody characteristics in bands 3 and 4 but not in bands 1 and 2. The candidate-returning magnitude difference constraints are labeled in Figure 2 and were compared with temperature-respective blackbody magnitude values in Figure 2 in black.

The queries returning the top 5% number of candidates were re-queried for right ascension and declination values. Because these queries returned relative spikes in candidates, they were assumed to be the queries holding brown dwarfs. Figures 3 through 9 display individual candidates as points in the 2D plane of the sky where the x-axis of each figure is the right ascension and the y-axis is the declination. The redder the object, the dimmer it is and therefore the farther away it is. The data shown in Figure 3 were assessed for a 2D and 3D isotropic distribution to ensure that the dwarf collection detected in WISE data from a spike in query returns was legitimate. To test for an isotropic distribution in 3D space, the band 1 magnitude data were grouped by brightness into 5 equal intervals where the brightest objects lay in interval 1 and the dimmest in interval 5. The dimmer the object, the farther away it was assumed to be. It was found that for dwarfs of temperature 200 - 450 K, the number of candidates significantly increased as interval number grew. In figure 10, this trend is evident except for after interval 4 for temperatures 250 - 450 K and after interval 3 for 500 K. This phenomenon was explained by the WISE limiting magnitude of 22 V[13], which caused the telescope to pick up some but not all of the candidates in the higher interval groups. Therefore, the figure confirmed the fact that more brown dwarfs were found farther from the earth than close to the earth, a distribution consistent with the geometric postulate that volume of space is proportional to the cube of the radius. The assessment depicted by Figure 4 therefore justified the isotropy of the brown dwarf distribution in 3D space.

To ensure that the candidates also followed an isotropic distribution in the 2D celestial plane, the average angular separation of candidates to their nearest neighbors was calculated for each temperature and plotted



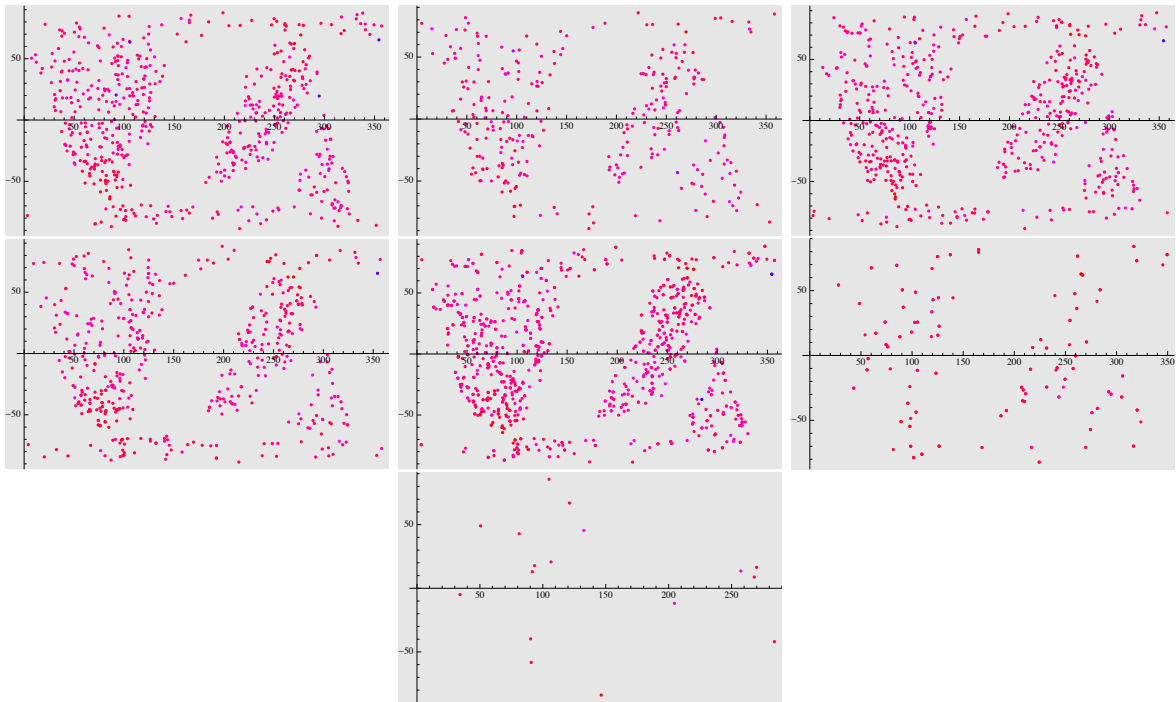


Figure 3: Candidates by Ra (x) Dec (y) Location Reddened Proportional to Apparent Magnitude Value (V): 200 K (top-left) 250 K (top-center) 300 K (top-right) 350 K (middle-left) 400 K (middle-center) 450 K (middle-right) 500 K (bottom-center)

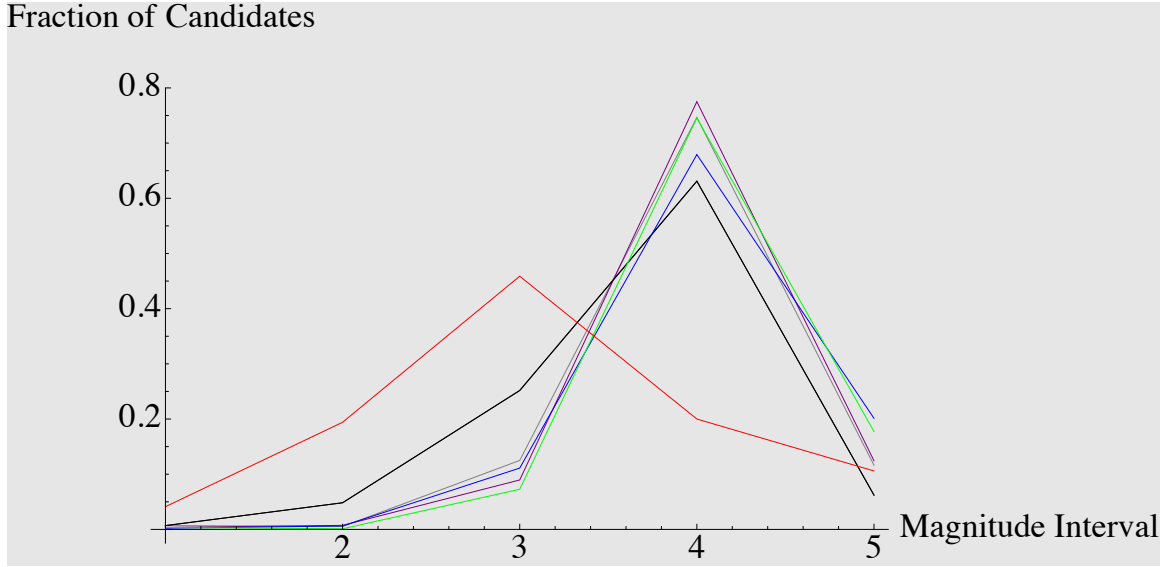


Figure 4: Plot of the fraction of candidates contained in Band 1 magnitude (distance) interval vs. the interval index. Color code: 250 K (green), 300 L (purple), 350 K (blue), 400 K (grey), 450 K (black) and 500 K (red)

Table 3: Monte Carlo Nearest Brown Dwarf Candidate Positional Coordinates and Temperatures

#	RA (°)	DEC (°)	T (K)
1	261.164	43.172	250
2	354.332	65.379	300-400
3	284.469	37.244	400
4	248.028	24.434	450

(Figure 5) in blue. The average plus the standard deviation was plotted in purple, the average minus the standard deviation was plotted in gray, the minimum degree separation in green, and the maximum degree separation in red. The plot (Figure 5) provided a quantitative confirmation of the qualitative 2D isotropy evident in the celestial plane distributions plotted for each of the temperatures in Figure 3.

From the spatial mapping of the candidate brown dwarfs from Figure 3, it was evident, as expected, that few brown dwarfs had exceptionally bright magnitudes, denoted by a blue or purple color. These brown dwarfs were labeled as the nearest brown dwarf candidates. The right ascension and declination of the nearest brown dwarf (the brightest) for each temperature range was collected and the candidate data are listed in Table 3.

## 4 Illustrations

The positional information of the eleven candidates from the blackbody query results and the five candidates from the Monte Carlo results was used to extract RGB\* FITS files. The FITS files if available for both 2MASS and WISE, were used to assess shift. Otherwise, the images were simply used to manually verify that the appearance of the object was consistent with the geometry of a spherical point source expected from a planet or brown dwarf (i.e. Figure 6). All sixteen candidates from both query runs passed this visual verification

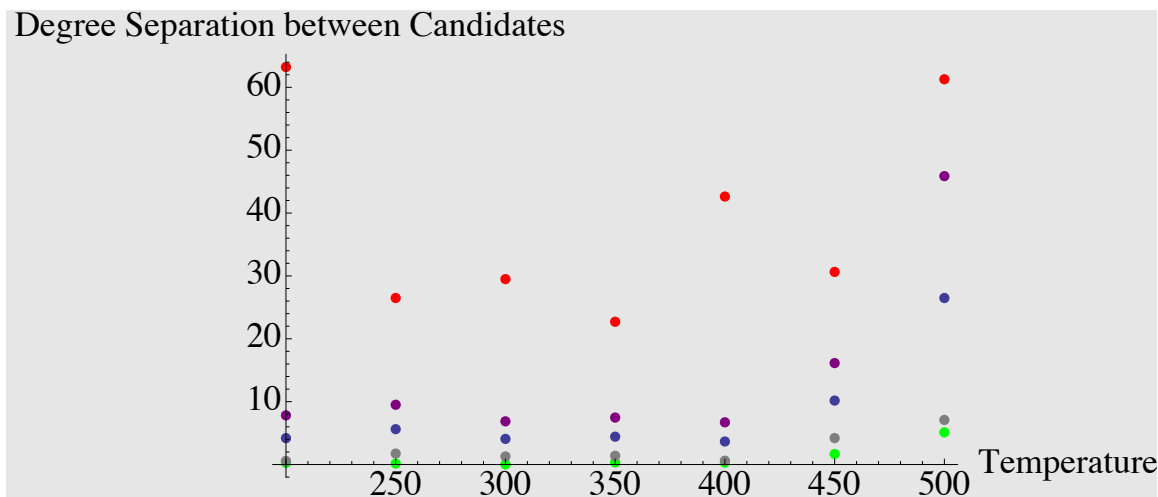


Figure 5: Plot of the Separation of Nearest Candidates (Degrees) vs Temperature

step.

## 5 Discussion: Spectral Analysis of Blackbody Candidates and Brown Dwarf Populations

To further comprehend the nature of the blackbody query candidates, spectral curve analysis was completed for the two candidates for Planet X as well as the nine candidates for extra-solar brown dwarfs. The correlation between the source spectra and temperature-respective blackbody spectra was quantitatively determined. The analysis of each point source consisted of a comparison between the actual number of electrons released per second by the WISE CCD due to the source and the theoretical number of electrons released per second by the CCD under the blackbody assumption. The theoretical value was calculated by evaluating Eq. 22 for each band pass  $n$  given the assumed  $T$  and  $d$  values from Table 3 and an  $r$  of  $1.0R_J$ . The actual number of electrons released per second was calculated by solving Eq. 23 for  $e_n^{experimental}$  for each band pass  $n$ .

$$e_n^{theoretical} = B_n(T, d, r) \quad (22)$$

$$M(e_n^{experimental}, B_n(T_v, d_v, r_v)) = M_{exp}^n \quad (23)$$

$$c_n = \frac{e_n^{experimental}}{e_n^{theoretical}} \quad (24)$$

It was found (Table 4) that all the spectra of the objects followed the blackbody functions diminished or augmented by a less-than-unity constant factor  $c$ . The constant factor was calculated by taking the average of  $c_1$ ,  $c_2$ ,  $c_3$ , and  $c_4$ , which were correlation values found for each band pass  $n$  using Eq. 24.

It was therefore concluded that candidates 2, 3, 4, and 6 through 11 were consistent with blackbodies because they radiated within 1.0% of ideal blackbodies of the same temperature, and that candidates 1 and 5 were approximate blackbodies, radiating within 15% of ideal blackbodies of the same temperature.

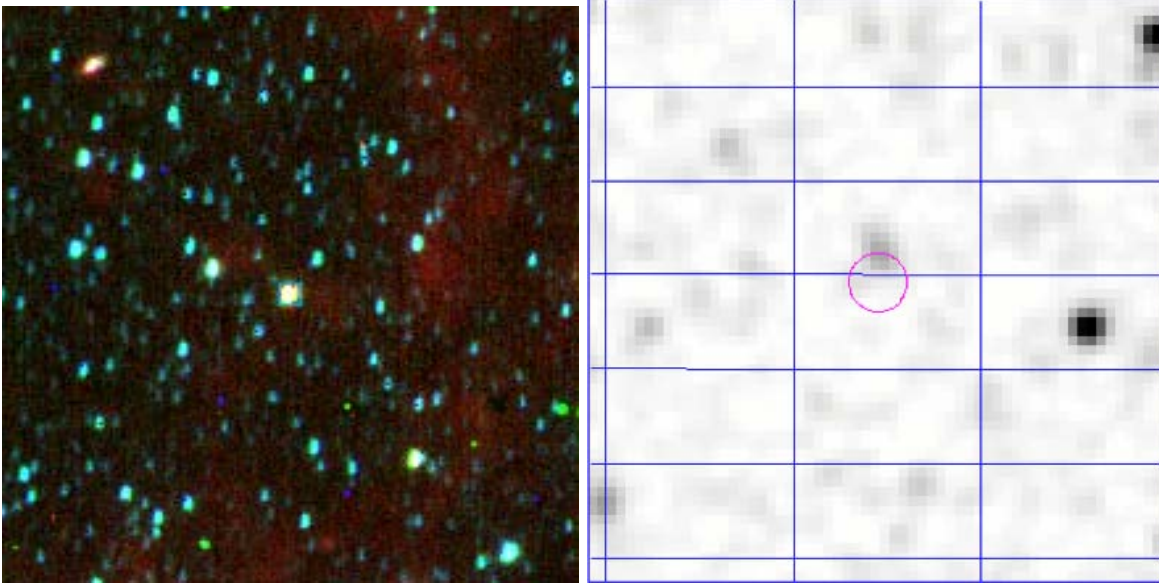


Figure 6: Centered FITS images for candidate # 5 in WISE (Composite of 4 bands) (left) and 2MASS (J Band\*) (right). Specific positional information from the FITS files was used to determine the exact shift. Assessment of the images with the naked eye was only used for verification of brown dwarf geometry.

Table 4: List of blackbody model correlation values  $c$  for each candidate.

#	Blackbody Correlation $c$
1	$0.862077 \pm 0.191683$
2	$1.00038 \pm 0.0510343$
3	$0.993943 \pm 0.0784415$
4	$1.00055 \pm 0.0484737$
5	$0.862077 \pm 0.191683$
6	$1.00038 \pm 0.0510343$
7	$1.00039 \pm 0.00820214$
8	$1.00028 \pm 0.0366681$
9	$1.00033 \pm 0.0145071$
10	$1.00022 \pm 0.00942987$
11	$1.00038 \pm 0.0510343$

Table 5: The ratio function coefficients for the form  $a\lambda^3 + b\lambda^2 + c\lambda + d$  where  $\lambda$  is wavelength

T (K)	a (1/cm)	b (1/cm)	c (1/cm)	d (1/cm)
200	$-4.136 \times 10^{10}$	$1.248 \times 10^8$	$-5.857 \times 10^4$	8.226
250	$-4.121 \times 10^{10}$	$1.254 \times 10^8$	$-6.309 \times 10^4$	9.638
300	$-5.801 \times 10^{10}$	$1.787 \times 10^8$	$-9.382 \times 10^4$	14.584
350	$-8.181 \times 10^{10}$	$2.554 \times 10^8$	$-1.432 \times 10^4$	23.402
400	$-5.771 \times 10^{10}$	$1.784 \times 10^8$	$-9.572 \times 10^4$	15.232
450	$-3.049 \times 10^{10}$	$9.088 \times 10^7$	$-4.106 \times 10^4$	5.751
500	$-1.061 \times 10^{10}$	$2.623 \times 10^7$	775.057	-1.731

Spectral investigation of the populations of brown dwarfs found in the Monte Carlo query results was performed through use of experimental magnitude values of candidates to deduce flux ratios. Because neither parallax data nor expected spectral models were available, complete deduction of the spectra of the brown dwarf populations could not be completed. Only the flux to band 1 flux ratio data were calculable by rearranging Eq. 16 as ratio functions described by Eq. 25-27.

$$\frac{f_2}{f_1} = \frac{v_2(\pi d_V^2) 10^{\frac{M_2}{-2.5}}}{\frac{v_1(\pi d_V^2)}{\pi d_0^2} 10^{\frac{M_1}{-2.5}}} = \frac{v_2 10^{\frac{M_2}{-2.5}}}{v_1 10^{\frac{M_1}{-2.5}}} \quad (25)$$

$$\frac{f_3}{f_1} = \frac{v_3 10^{\frac{M_3}{-2.5}}}{v_1 10^{\frac{M_1}{-2.5}}} \quad (26)$$

$$\frac{f_4}{f_1} = \frac{v_4 10^{\frac{M_4}{-2.5}}}{v_1 10^{\frac{M_1}{-2.5}}} \quad (27)$$

For each temperature between 200 and 500 K, functions of wavelength were fit to the ratio data and compared with the ratio functions expected from a standard blackbody. The third order polynomial flux ratio functions for each temperature are given in Table 5.

The plots of the polynomial functions (Figure 7) revealed that the interstellar populations of brown dwarfs had spectra that were significantly different from standard blackbody spectra of the same temperature. While for temperatures 200 K and 250 K, expected blackbody flux ratios exceeded experimental values, for temperatures 300 K - 500 K, the opposite was true. Moreover, the plotting of the flux ratio data points revealed qualitatively that in band 3 (7.5 – 16.5  $\mu\text{m}$ ) data deviated more from the ratio function than in band 1, 2, or 4 data. This phenomenon made band 3 the frequency range in which the hypothesis that all browns dwarfs have identical spectra was least supported. Because the query process mandated only 20% deviation from blackbody values in bands 3 and 4, consistent clumps of ratio points in bands 1 and 2 alone provided support for the identical-spectra hypothesis.

## 6 Conclusions

The conducted research presented sixteen new candidates for interstellar brown dwarfs, two of which are candidates for the postulated solar system object "Planet X" described in literature by Matese and Whitmire19. Eleven of the candidates were found by querying the WISE preliminary release source catalog with magnitude constraints derived from blackbody theory. The remaining five nearest-brown-dwarf candidates were found by querying the catalog with Monte Carlo variants of the blackbody standards. Spectral analysis of the blackbody candidates presented a high correlation between the spectra of candidates and expected blackbody spectra. For the six Monte Carlo temperature-indexed brown dwarf populations, the ratios of

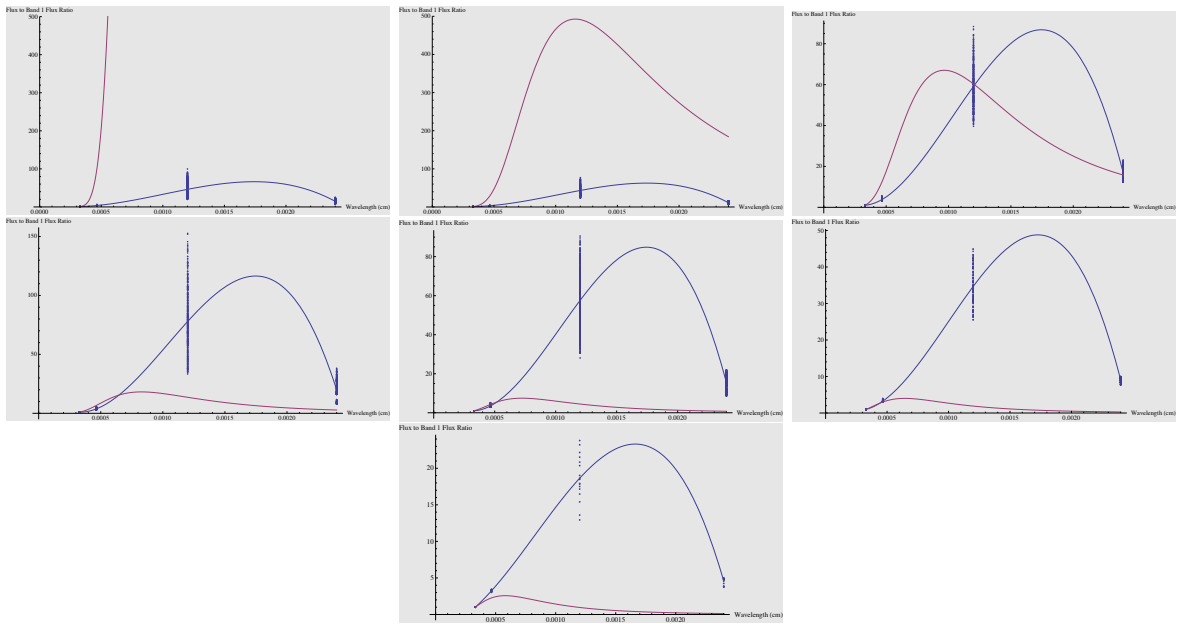


Figure 7: Plots of Flux Ratio Functions fitted to data at Given Wavelength vs. Wavelength for Brown Dwarf Population (Blue), Respective Temperature Blackbody Ratio Function (Red). 200 K (top-left) 250 K (top-center) 300 K (top-right) 350 K (middle-left) 400 K (middle-center) 450 K (middle-right) 500 K (bottom-center)

the spectra to band 1 flux values were also modeled, showing imminent divergence from blackbody spectral ratios at all investigated temperatures 200 K through 500 K. The full spectral information for these five candidates will be known once distance data are known after proper motion and parallax tests upon the WISE second epoch data release. At that time, the fidelity of all sixteen candidates will also be confirmed provided that the candidates display significant positional shift. If confirmed, the candidates will constitute a startling 21st century astronomical advance.

## Glossary

**Apparent Magnitude** A measure of brightness measured in  $V$ . It is proportional to the negative logarithm of the ratio of the measured flux of the object to the flux of Vega. An object with a large positive apparent magnitude value will be dim.

**ASCII** American Standard Code for Information Interchange.

**Brown Dwarf** Objects of temperatures too low to maintain hydrogen fusion reactions. Brown dwarfs vary in mass from 1 to 100  $M_J$  but have a standard radius of  $R_J$ .

**Isotropy** Describes a uniform distribution throughout a set of spatial dimensions

**J Band of 2MASS** Lowest wavelength band of 2MASS ranging from  $1.0\mu\text{m}$  -  $1.4\mu\text{m}$ .

**Monte Carlo generation** A process in which a randomization algorithm is applied to a theoretical model to simulate natural deviation.

**RGB** 3 color (red, green, blue) imaging

**$R_J$  ,  $M_J$**  The radius and mass of Jupiter respectively.

**SQL** Structured Query Language

**w and b** Synonymous with "band" magnitude. For instance,  $w_1$  or  $b_1$  refer to band 1.

**WISE and 2MASS Limiting Magnitudes** Refers to the maximum apparent magnitudes (minimum brightness / maximum dimness) each telescope can detect.

**WISE bands** The four electromagnetic wavelength ranges in which the four WISE filters let in radiation. Band 1 ranges from  $2.8\mu\text{m}$  -  $3.8\mu\text{m}$ , Band 2,  $4.1\mu\text{m}$  -  $5.1\mu\text{m}$ , Band 3,  $7.5 - 16.5\mu\text{m}$ , and Band 4,  $20 - 28\mu\text{m}$

## References

- [1] Luhman, K. L., A. J. Burgasser, and J. J. Bochanski. "Discovery of a Candidate for the coolest known Brown Dwarf." *The Astrophysics Journal* (March 2011). <http://arxiv.org/abs/1102.5411>.
- [2] Matese, John J., and Daniel P. Whitmire. "Persistent Evidence of a Jovian Mass Solar Companion in the Oort Cloud." *Icarus* (April 2010).
- [3] Scholz, Ralf-Dieter, G. Bihain, O. Schnurr, and J. Storm. "Two very nearby ( $d \sim 5$  pc) ultracool brown dwarfs detected by their large proper motions from WISE, 2MASS, and SDSS data." *Astronomy and Astrophysics* (May 2011). <http://arxiv.org/abs/1105.4059v2>.
- [4] Burrows, Adam, David Sudarsky, and Jonathan Lunine. "Beyond the T Dwarfs: Theoretical Spectra, Colors, and Detectability of the Coolest Brown Dwarfs." *Astrophysical Journal* (June 2003). <http://arxiv.org/abs/astro-ph/0304226v2>.

- [5] Burgasser, Adam J., Michael C. Cushing, J. Davy Kirkpatrick, Christopher R. Gelino, Roger L. Griffith, Dagny L. Looper, Christopher Tinney, Robert A. Simcoe, John J. Bochanski, and Michael F. Skrutskie. "FIRE Spectroscopy of Five Late-type T Dwarfs Discovered with the Wide-field Infrared Survey Explorer." *Astrophysical Journal* (April 2011). <http://arxiv.org/abs/1104.2537v1>.
- [6] Mainzer, A., J. Bauer, T. Grav., J. Masiero, R. M. Cutri, J. Dailey, P. Eisenhardt, R. S. McMillan, E. Wright, R. Walker, and R. Jedicke. "Preliminary Results from NEOWISE: An Enhancement to the Wide-field Infrared Survey Explorer for Solar System Science." *Astrophysical Journal* (February 2011). <http://arxiv.org/abs/1102.1996v1>.
- [7] Bilir, S., S. Karaali, N. D. Dagtekin, O. Onal, E. Yaz, B. Coskunoglu, and A. Cabrera-Lavers. "Transformations between WISE, 2MASS, SDSS and BVRI photometric systems: I. Transformation equations for dwarfs." *Monthly Notices of the Royal Astronomical Society* (July 2011). <http://arxiv.org/abs/1107.1350v1>.
- [8] "WISE Preliminary Release Catalog Search Engine." Infrared Science Archive (NASA/Caltech). [http://irsa.ipac.caltech.edu/cgi-bin/Gator/nph-scan?mission=irsa&submit=Select&projshort=WISE\\_PRELIM](http://irsa.ipac.caltech.edu/cgi-bin/Gator/nph-scan?mission=irsa&submit=Select&projshort=WISE_PRELIM).
- [9] "NASA / IPAC Infrared Science Archive." NASA / IPAC Infrared Science Archive. [http://irsa.ipac.caltech.edu/applications/wise/#id=Hydra\\_wise\\_wise\\_1&projectId=wise&startIdx=0&pageSize=0&shortDesc=Position&isBookmarkAble=true&isDrillDownRoot=true](http://irsa.ipac.caltech.edu/applications/wise/#id=Hydra_wise_wise_1&projectId=wise&startIdx=0&pageSize=0&shortDesc=Position&isBookmarkAble=true&isDrillDownRoot=true).
- [10] Mathematica. 8th ed. Application. Wolfram Mathematica.
- [11] WISE Preliminary Release Explanatory Supplement. <http://wise2.ipac.caltech.edu/docs/release/prelim/>.
- [12] Logger Pro. 3rd ed. Application, version 3.5.0. Vernier Software & Technology.
- [13] 2MASS Explanatory Supplement. <http://www.ipac.caltech.edu/2mass/releases/allsky/doc/explsup.html>.